

PELDOR distance fingerprinting of the octameric outer-membrane protein Wza from *Escherichia coli*.

Gregor Hagelueken¹, W. John Ingledeu¹, Hexian Huang¹, Biljana Petrovic-Stojanovska¹, Chris Whitfield², Hassane ElMkami³, Olav Schiemann^{1,*}, James H. Naismith^{1,*}

¹Centre for Biomolecular Sciences, University of St Andrews, Fife KY16 9RH, UK.

²Department of Molecular and Cellular Biology, University of Guelph, Ontario N1G 2W1, Canada

³School of Physics and Astronomy, University of St Andrews, Fife KY16 9RH, UK

Supporting information

Table of contents:

1. Protein expression & purification.....	6
1.1. Full length Wza.....	6
1.2. Wza24-345 (sWza)	6
1.3. Verification of octameric state of sWza.....	6
1.4. Spin labelling.....	7
2. PELDOR.....	7
2.1. Sample Preparation	7
2.2. PELDOR Measurements	7
3. PELDOR Data.....	7
3.1. Wza Q335C	9
3.2. Wza G58C	10
3.3. sWza Q335C.....	11
3.4. sWza G58C.....	12
3.5. sWza Q143C.....	13
3.6. sWza N78C.....	14
3.7. Spin counting.....	15
4. Crystallographic methods for the sWza and spin labelled sWza structures	17
4.1. Crystallization.....	17
4.2. Data collection & refinement	17
4.3. Crystallographic data	18
5. References.....	18



Protein expression & purification

Full length Wza

The full length Wza protein from *Escherichia coli* was expressed and purified as described.^[15] Mutants G58C and Q335C were prepared using the Quickchange site-directed mutagenesis kit (Stratagene). 1 mM DTT was used throughout the purification procedure in order to keep the introduced thiol sidechain in a reduced state.

Wza24-345 (sWza)

Plasmid pWQ126^[16] and oligonucleotides wza24-345fwd: 5'-GGAGGAGGTACCGACAATCATCCCTGGTCAGGG-3' and wza24-345rev: 5'-GCCGCCGAGCTCTTAGTTTGGCCATCTCTTAATGTATCG-3' were used to amplify region 24-359 of *wza* by PCR. The PCR product was cloned into plasmid pBADHISTEV (Huanting Liu, BMS, The University of St. Andrews, personal communication) using restriction enzymes *KpnI* and *SacI*. The Quickchange site-directed mutagenesis kit was then used to introduce a stop codon at position 346. For expression, the pBADHISTEV-wza24-345 construct was transformed into LMG194 cells (Invitrogen). Typically, 10 l LB Medium were supplemented with 100 µg/ml ampicillin and inoculated with 100 ml of an overnight culture. Once the culture achieved OD₆₀₀ of ~0.5, gene expression was induced by adding 0.02% L-arabinose and incubation was continued overnight at 15°C. Cells were harvested, resuspended in 50 mM Tris-Cl pH8, 100 mM NaCl (buffer A) and disrupted using a sonicator. The insoluble material was removed by centrifugation and the soluble fraction containing Wza24-345 was incubated for 1h at 4°C with Ni-NTA resin equilibrated in buffer A. The resin was washed with 200 ml buffer A containing 200 mM imidazole and eluted with buffer A containing 500 mM imidazole. The Ni-NTA elution fractions were then directly loaded onto a HiTrapQ HP column (GE Healthcare) and eluted with a steep NaCl gradient (buffer A + 100-1000 mM NaCl for 5 column volumes. The sWza-containing fractions (elution at approximately 500 mM NaCl) were pooled and supplemented with 0.5 mM EDTA, 5 mM DTT, and 2 mg TEV protease. The TEV cleavage was performed overnight at 4°C. Purification was finished by loading the reaction mixture onto a Superdex200 16/60 column (GE Healthcare) with buffer A as eluant. For mutants G58C, N78C, Q143C and Q335C, 5 mM DTT was added in order to keep the introduced thiol sidechain in a reduced state. The protein was stored at -80°C.

Verification of octameric state of sWza

Blue-native PAGE and gel filtration experiments were used to verify that sWza has the same octameric secondary structure as the full length Wza. Additionally, we crystallized sWza (see below) and found that the structure of sWza is essentially identical to the structure of full-length Wza.^[3]

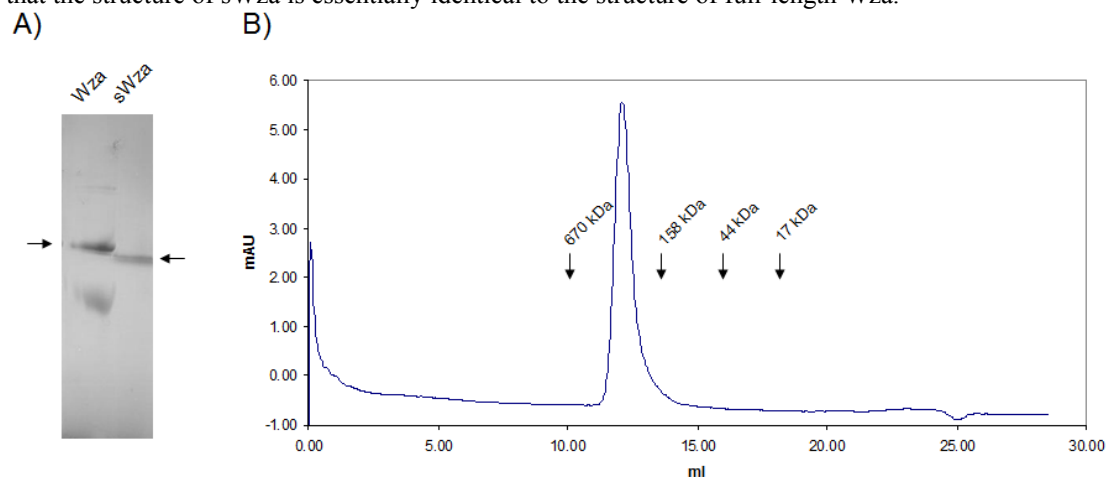


Figure S1: Verification of octameric state of sWza. A) Blue native PAGE (Invitrogen) of Wza and sWza. The bands for Wza and sWza are indicated by arrows. The gel was prepared according to the recommendations of the manufacturer. B) Gel filtration profile of sWza. A Superdex200 10/300 GL column (GE Healthcare) was used for the experiment. The column was calibrated with standard proteins (arrows, Bio-RAD). sWza elutes at a volume corresponding to a molecular weight of ~298 kDa (calculated MW for octameric sWza: 286 kDa).

Spin labelling

DTT was removed from the Wza and sWza samples by gel-filtration with buffer A (see above). The protein was concentrated to 30 μM and incubated overnight at 4°C with 300 μM MTSSL (Toronto Research). Excess MTSSL was then removed by gel-filtration with PD-10 columns (GE Healthcare).

PELDOR

Sample Preparation

Samples at a concentration of 250 μM were prepared in TES D₂O buffer (10 mM, pH 7.59) containing 50% ethylene glycol as cryoprotectant. Samples of Wza also contained 0.008 % DDM. Aliquots of 100 μl were transferred into quartz EPR tubes and quickly frozen by immersing the tubes into a freezing mixture (methylenecyclohexane : isopentane = 1 : 4) cooled to -80°C with liquid nitrogen. Samples were degassed by several pump-thaw cycles and finally kept under an atmosphere of nitrogen.

PELDOR Measurements

All PELDOR spectra were recorded on a Bruker ELEXSYS E580 pulsed X-band EPR spectrometer, with a standard flex line probe head housing a dielectric ring resonator (MD4). The instrument was equipped with a continuous flow helium cryostat (CF935) and temperature control system (ITC 502), both from Oxford instruments. The second microwave frequency was coupled into the microwave bridge using a commercially available setup from Bruker. All pulses were amplified via a pulsed travelling wave tube (TWT) amplifier (117X) from Applied Systems Engineering. The resonator was over-coupled to a quality factor Q of about 50. PELDOR experiments were performed with the pulse sequence $\pi/2(\nu_A)-\tau_1-\pi(\nu_A)-(\tau_1+t)-\pi(\nu_B)-(\tau_2-t)-\pi(\nu_A)-\tau_2$ -echo. The detection pulses (ν_A) were set to 16 ns for the $\pi/2$ and 32 ns for the π pulses and applied at a frequency 80 MHz higher than the resonance frequency of the resonator. The pulse amplitudes were chosen to optimize the refocused echo. The $\pi/2$ -pulse was phase-cycled to eliminate receiver offsets. The pump pulse (ν_B) with a length of 28 ns was set at the resonance frequency of the resonator. The field was adjusted such that the pump pulse is applied to the maximum of the nitroxide spectrum, where it selects the central $m_1 = 0$ transition of A_{zz} together with the $m_1 = 0, \pm 1$ transitions of A_{xx} and A_{yy} . The pulse amplitude was optimized to maximize the inversion of a Hahn-echo at the pump frequency. All PELDOR spectra were recorded at 50 K with an experiment repetition time of 4 ms, a video amplifier bandwidth of 20 MHz and an amplifier gain of 54 dB. τ_1 was set to 380 ns and τ_2 varied from 2500 to 6000 ns. About 300 scans were accumulated with time increments Δt of 8 ns or 16 ns giving an approximate measurement time of 18 to 48 hours necessary to obtain a signal-to-noise ratio > 200:1. Proton modulation was suppressed by addition of 8 spectra of variable τ_1 with a $\Delta\tau_1$ of 8 ns.^[17] The obtained time traces were divided by a mono-exponential decay to eliminate intermolecular contributions and renormalized. Distance distributions were obtained from the background corrected data by using the program DeerAnalysis developed by Gunnar Jeschke.^[18]

PELDOR Data

The following time traces were all run with a short and a long τ_2 and a $\Delta\tau$ of 8ns and 16ns, respectively, in order to achieve a good resolution for the short range distances and a still reasonable measuring time for the longer distances. The lengths of the time traces were chosen such that they are longer than a period of the longest distance measured, to avoid artifacts in the distance distributions. The effect of too short time windows on long distances can nicely be seen in all cases; distances 1-3 are shifted in each case to shorter distances.

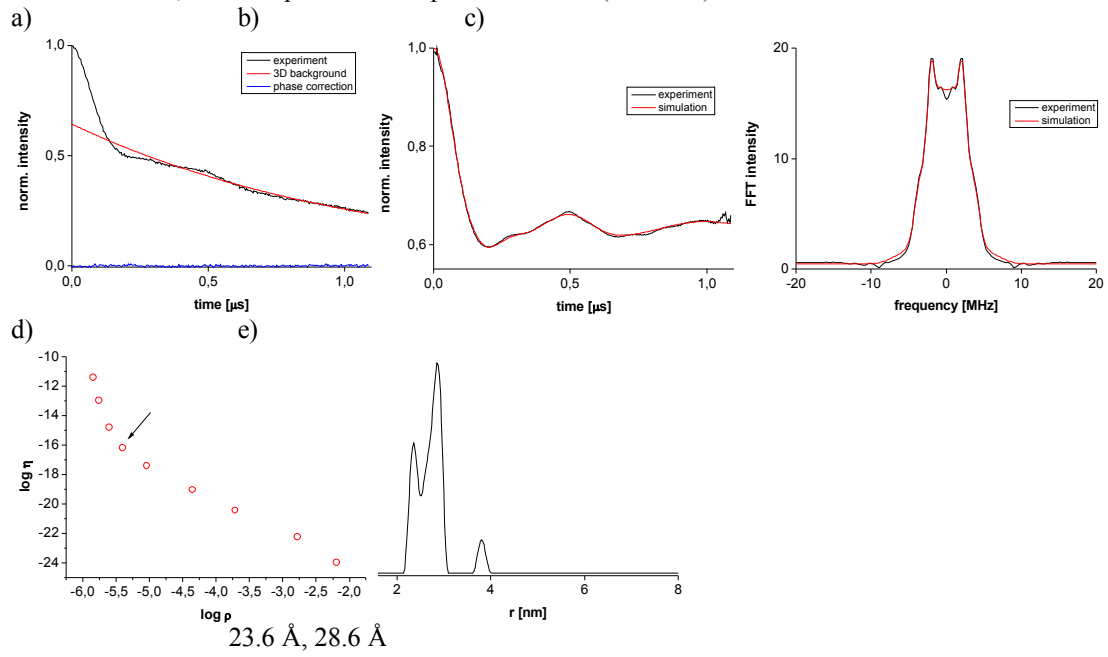
With respect to the inability to detect the long distances 1-4 and 1-5, the histogram in Figure 3 in the main text gives an additional reason why these are not resolved in the PELDOR data. The observed broad distance distribution translates into fast modulation damping, further complicating the separation of these signals from the intermolecular background.

Finally and in agreement with the crystal structure, the five-membered ring of both nitroxides can freely rotate around the carbon single bond, which gives enough orientation averaging to allow for an analysis based on the program DeerAnalysis as shown previously on systems of similar rigidity.^[6] This is also confirmed by varying the position of the detection sequence on the nitroxide spectrum (data not shown).

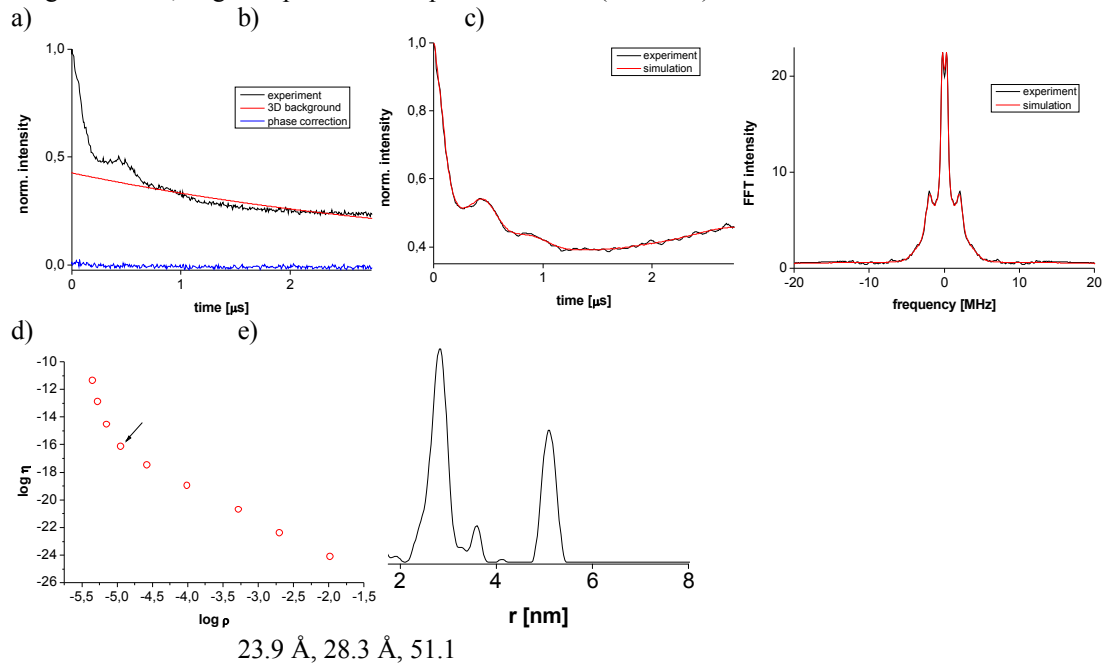
In the following, figures, a) represents the original time traces (black line) phase corrected and normalised to 1. The red line is the 3D background fitted to the experimental data and the blue line is the imaginary part after phase correction. b) The black line is the experimental time trace after background division overlaid with the simulation (red line). c) The Fourier transform spectra from b). d) The L-curve, with the alpha value taken to generate the distance distribution indicated by an arrow. e) The distance distribution and underneath the distances of the main peaks. In the main text, the short distances are taken from the short time traces and the longer ones from the long time traces.

Wza Q335C

short time trace, small step width for dipolar evolution ($\Delta\tau = 4\text{ns}$)

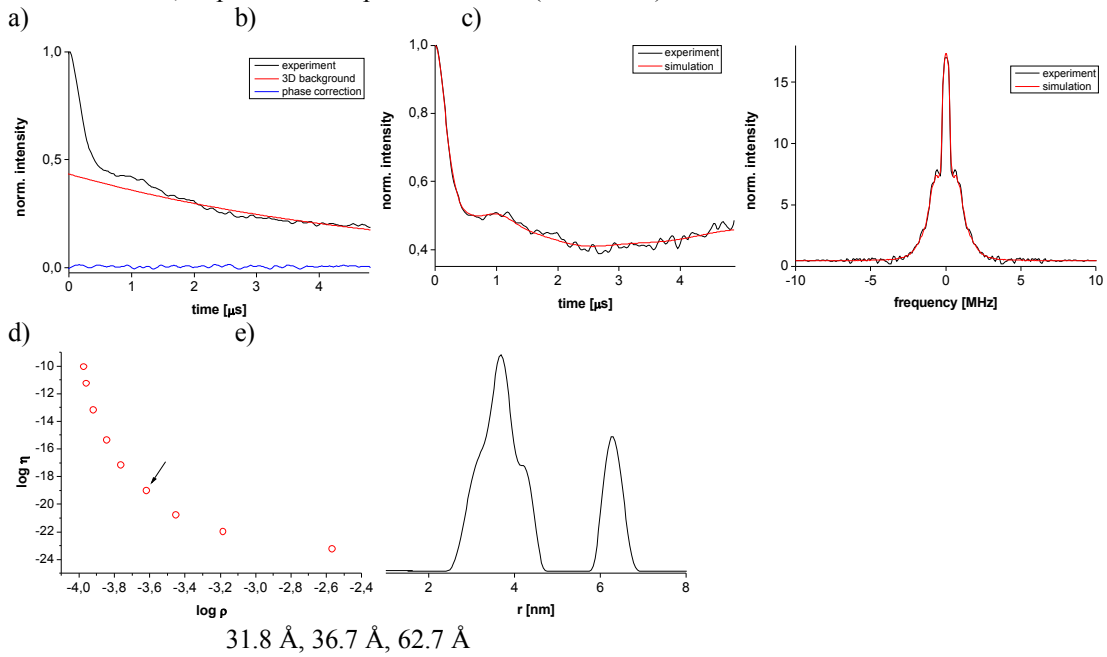


long time trace, larger step width for dipolar evolution ($\Delta\tau = 8\text{ns}$)

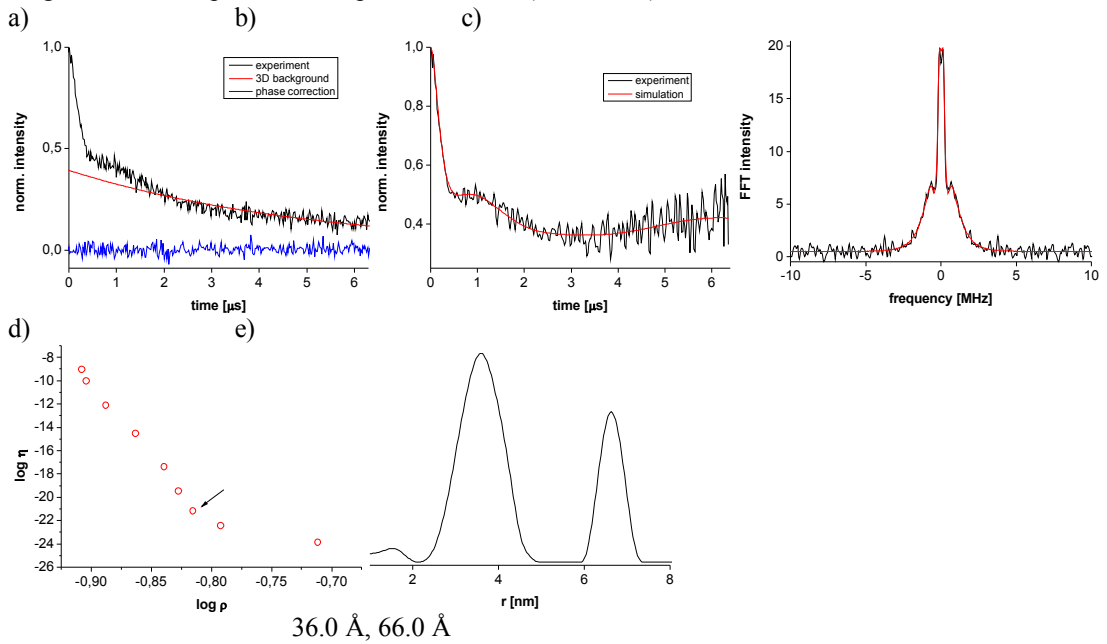


Wza G58C

short time trace, step width for dipolar evolution ($\Delta\tau = 20$ ns)

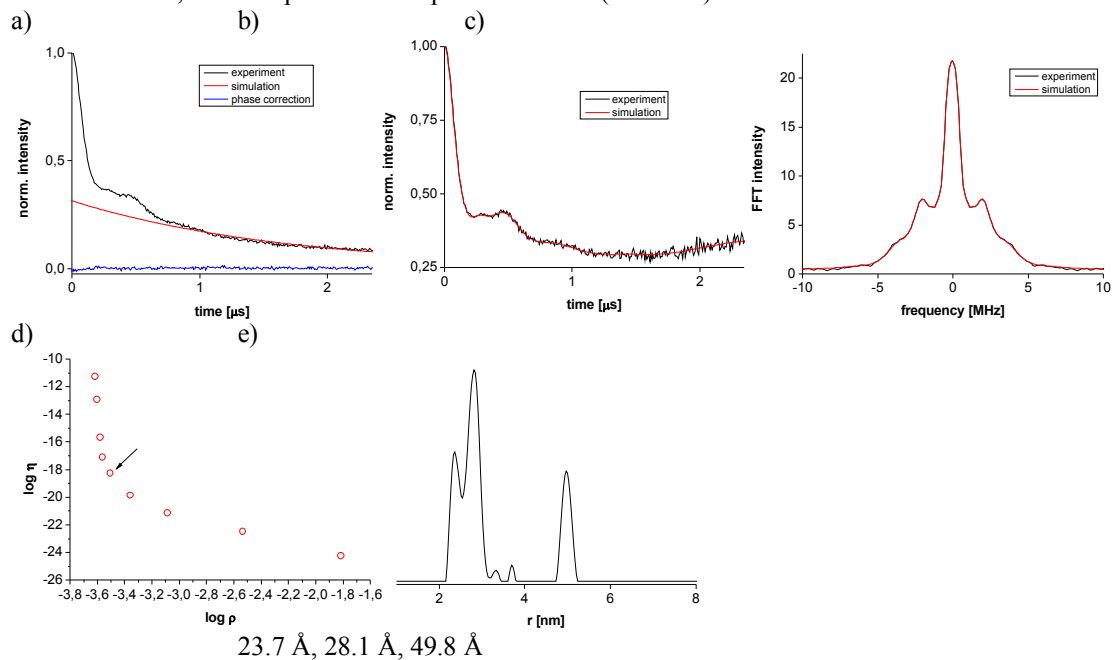


long time trace, step width for dipolar evolution ($\Delta\tau = 20$ ns)

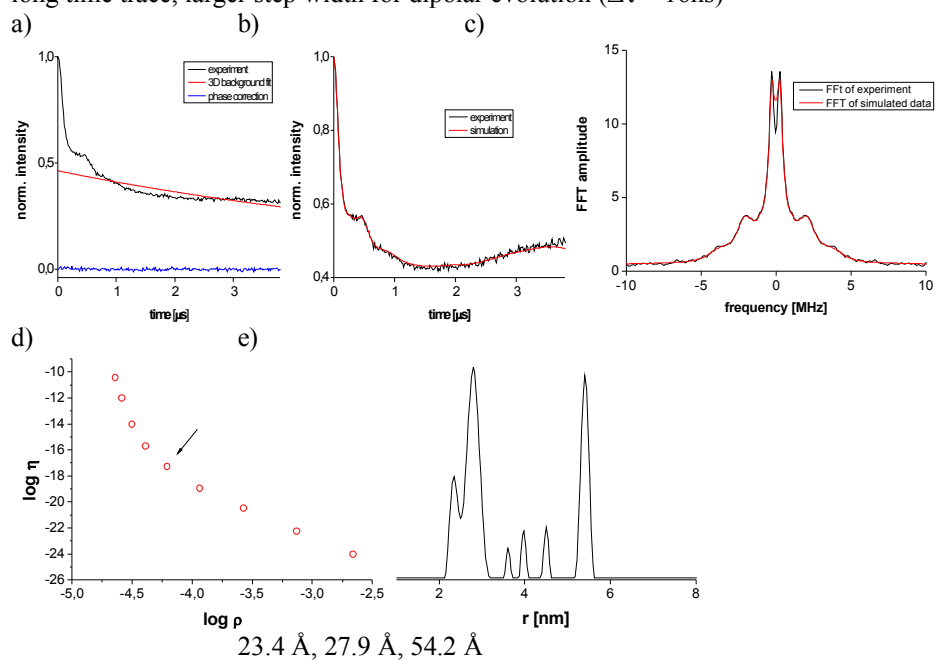


sWza Q335C

short time trace, small step width for dipolar evolution ($\Delta\tau = 8\text{ns}$)

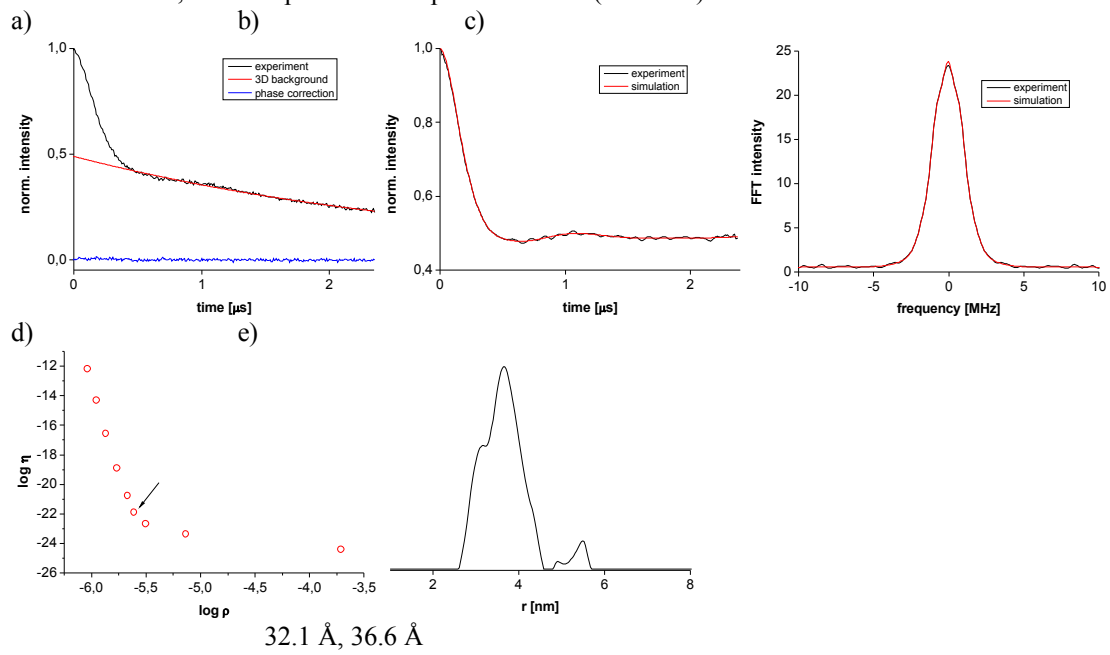


long time trace, larger step width for dipolar evolution ($\Delta\tau = 16\text{ns}$)

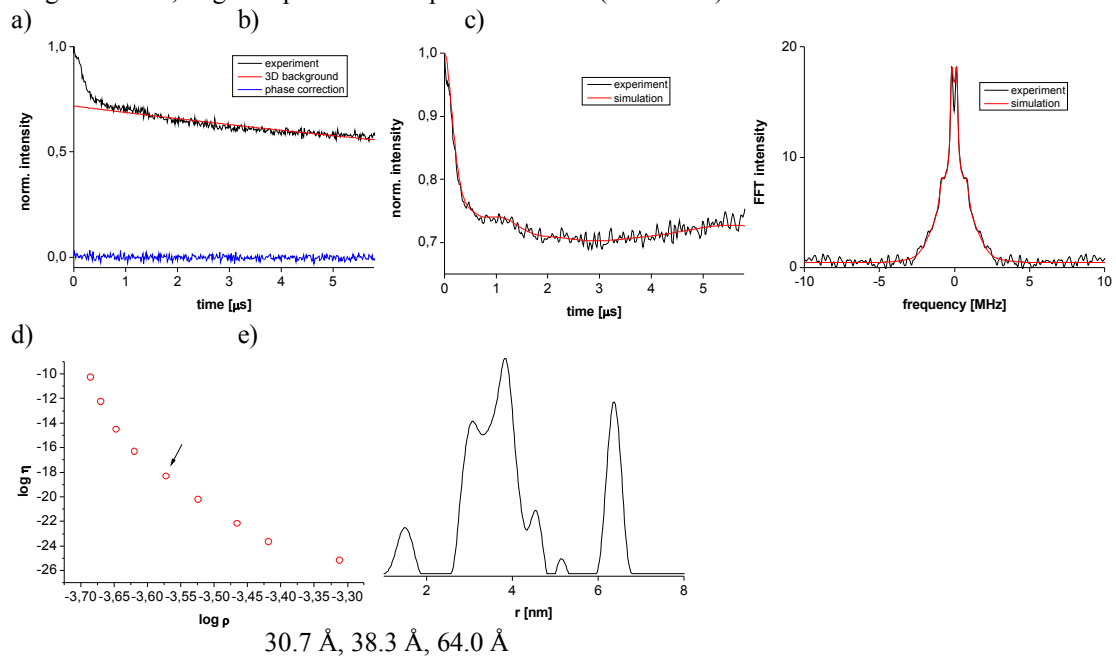


sWza G58C

short time trace, small step width for dipolar evolution ($\Delta\tau = 8\text{ns}$)

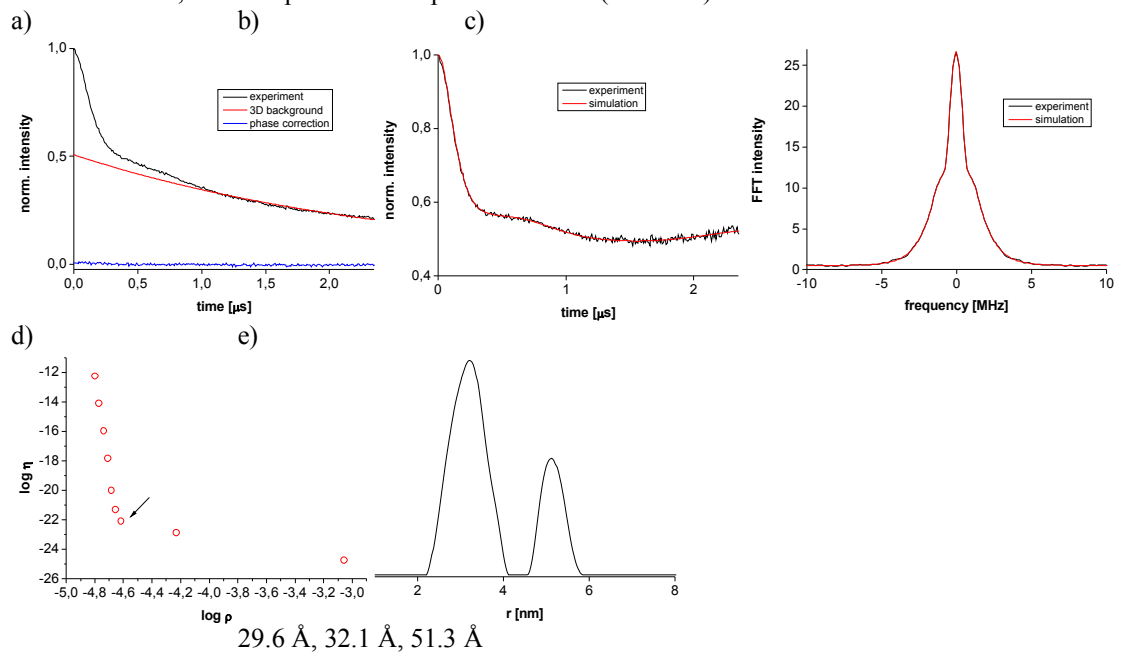


long time trace, larger step width for dipolar evolution ($\Delta\tau = 16\text{ns}$)

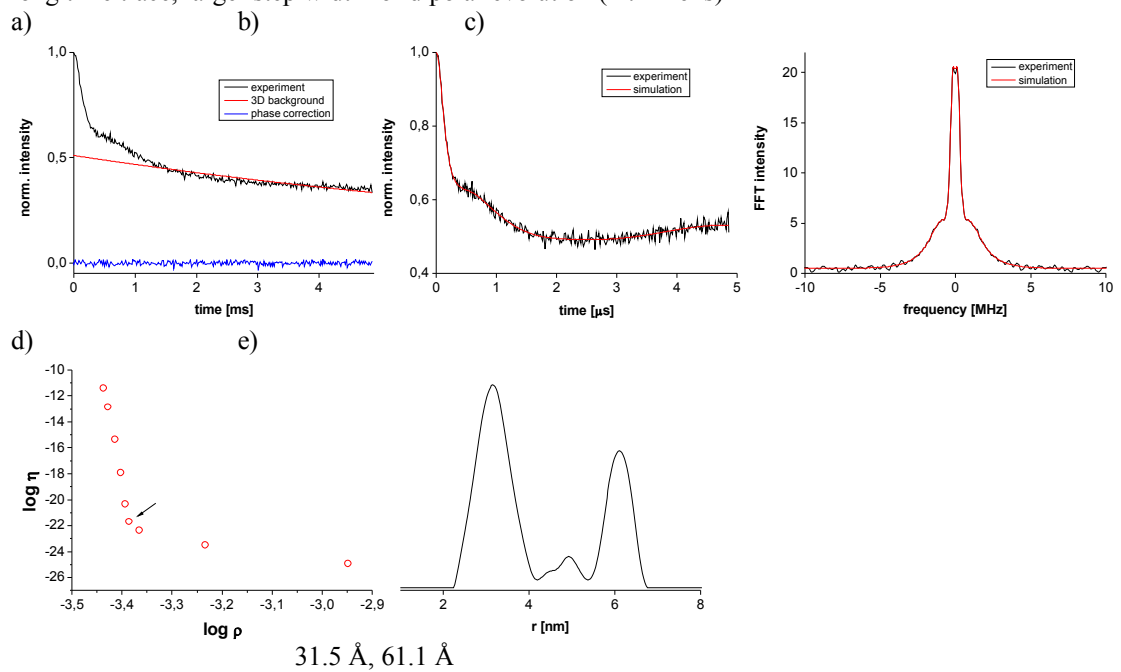


sWza Q143C

short time trace, small step width for dipolar evolution ($\Delta\tau = 8\text{ns}$)

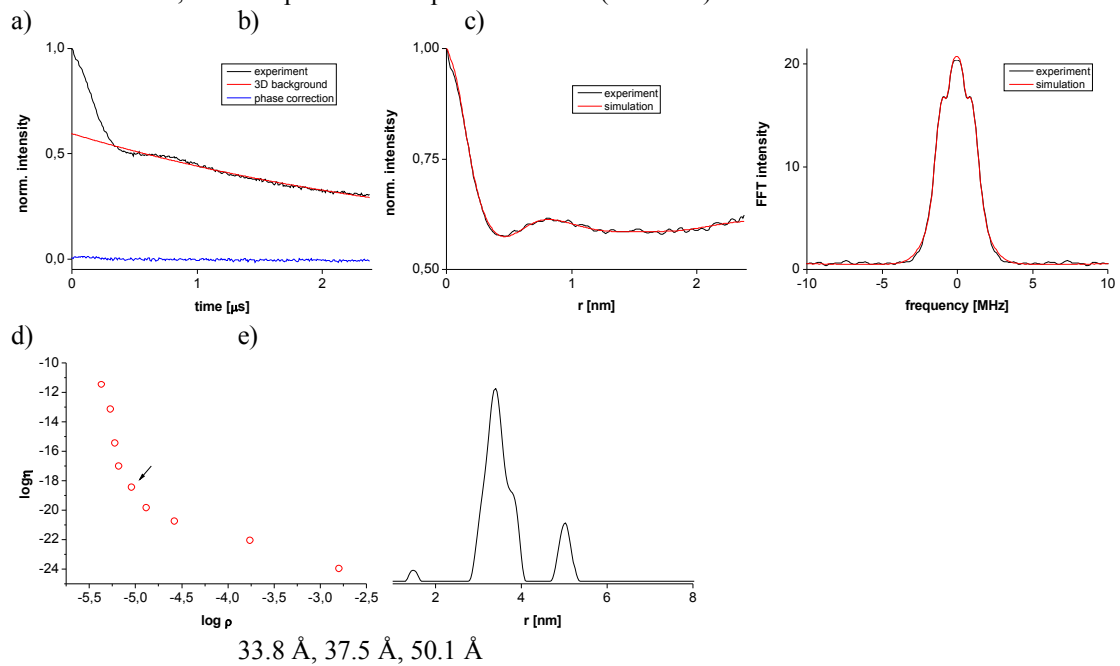


long time trace, larger step width for dipolar evolution ($\Delta\tau = 16\text{ns}$)

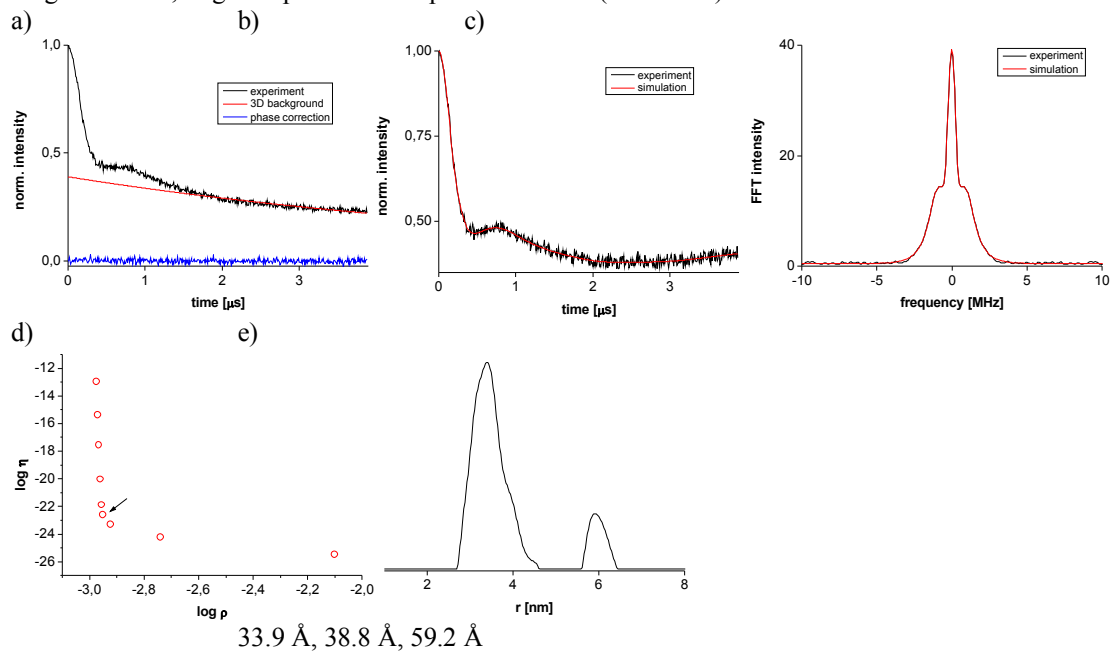


sWza N78C

short time trace, small step width for dipolar evolution ($\Delta\tau = 8\text{ns}$)



long time trace, larger step width for dipolar evolution ($\Delta\tau = 16\text{ns}$)



Spin counting

The modulation depth parameters λ gathered for different lengths t of the PELDOR pulse sequence are collected in Table S1 for sWza_{Q335C} and sWza_{N78C}. The plot of these data and their fits are shown in Figure S2. Extrapolating the fits back to $t = 0$, yields $\lambda = 0.94$ and 0.84 for sWza_{Q335C} and sWza_{N78C}, respectively. This is in agreement with the values of 0.94 and 0.85 calculated assuming a labeling efficiency of 85% and 65% for sWza_{Q335C} and sWza_{N78C}, respectively (Table S2). The basis for the calculation is equation (1)^[10] and common statistics. λ for a pure biradical sample in D₂O was set to 0.4 , commonly achieved in our hands with the spectrometer settings outlined above.

$$1 - \lambda = V_{\lambda} = \sum_i x_i V_{\lambda,i} \quad (1)$$

We do not claim that we are able to distinguish an spin-octamer from a spin-heptamer or spin-hexamer. However, this analysis proves that the small modulation depth observed at longer time windows, and corresponding rather to a spin-dimer than a spin-octamer, can be traced back to the different relaxation times of octamers carrying different numbers of spin labels.

Table S1. Modulation depth parameter λ for different lengths of the PELDOR pulse sequence for sWza_{Q335C} and sWza_{N78C}.

sWza _{Q335C}		sWza _{N78C}	
t [ns]	λ	t [ns]	λ
7760	0.60	8760	0.57
5760	0.63	5760	0.58
2360	0.67	3760	0.62
1360	0.74	2160	0.67

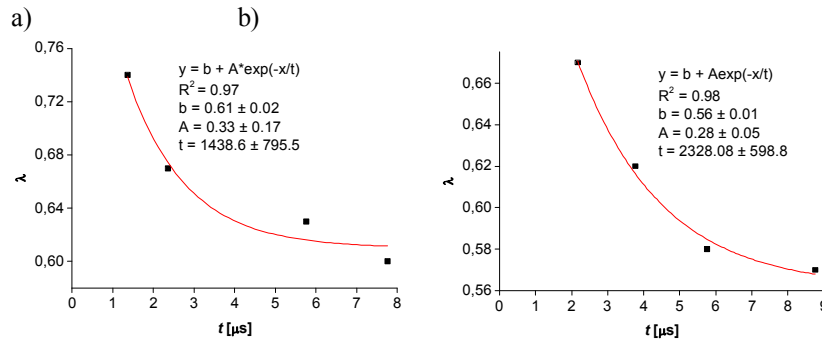


Figure S2: Plot and fit of λ and t for a) sWza_{Q335C} and b) sWza_{N78C}. The equations obtained for each fit are shown in the respective plots and are those used for the back extrapolation. Within each set of these measurements the same coupling was used and the sample was not removed during measurements.

Table S2. Calculated values for λ in dependence of the label degree.

spins realisations	0 1	1 8	2 28	3 56	4 70	5 56	6 28	7 8	8 1	Σ	
probability for 90% label degree (%)	1,00E-06	7,20E-05	2,27E-03	4,08E-02	4,59E-01	3,31E+00	1,49E+01	3,83E+01	4,30E+01	1,00E+02	
probability for 85% label degree (%)	2,56E-05	1,16E-03	2,30E-02	2,61E-01	1,85E+00	8,39E+00	2,38E+01	3,85E+01	2,72E+01	1,00E+02	
probability for 80% label degree (%)	2,56E-04	8,19E-03	1,15E-01	9,18E-01	4,59E+00	1,47E+01	2,94E+01	3,36E+01	1,68E+01	1,00E+02	
probability for 70% label degree (%)	6,56E-03	1,22E-01	1,00E+00	4,67E+00	1,36E+01	2,54E+01	2,96E+01	1,98E+01	5,76E+00	1,00E+02	
probability for 65% label degree (%)	2,25E-02	3,35E-01	2,17E+00	8,08E+00	1,88E+01	2,79E+01	2,59E+01	1,37E+01	3,19E+00	1,00E+02	
xV_λ 100% label degree	----	1,00	0,60	0,36	0,22	0,13	0,08	0,05	0,03	ΣxV_λ	λ
xV_λ 90% label degree	----	7,2E-07	1,4E-05	1,5E-04	9,9E-04	0,004	0,012	0,018	0,012	0,047	0,953
xV_λ 85% label degree	----	0,000	0,000	0,001	0,004	0,011	0,018	0,018	0,008	0,060	0,940
xV_λ 80% label degree	----	0,000	0,001	0,003	0,010	0,019	0,023	0,016	0,005	0,076	0,924
xV_λ 70% label degree	----	0,001	0,006	0,017	0,029	0,033	0,023	0,009	0,002	0,120	0,880
xV_λ 65% label degree	----	0,003	0,013	0,029	0,041	0,036	0,020	0,006	0,001	0,149	0,851

Crystallographic methods for the sWza and spin labelled sWza structures

Crystallization

For crystallization by vapour-diffusion methods, sWza and sWza_{Q335C}/MTSSL were concentrated to 9.5 mg/ml and mixed 2:1 with a reservoir solution consisting of 0.1 M HEPES pH 7.1 and 0.2 M CaCl₂ and 19% PEG 400. Large (200 μm) cube shaped crystals of space group P2₁2₁2 grew after 1-2 days.

Data collection & refinement

Prior to data collection, crystals were frozen in reservoir solution supplemented with 30% PEG 400. Diffraction data sets were collected in-house using Cu-Kα radiation and a Saturn 944+ CCD detector. The data were indexed and processed and scaled in space group P2₁2₁2 using the HKL2000 package.^[19] The structure was solved using the PHASER suite for molecular replacement.^[20] A single monomer of the full length Wza structure^[3] (including residues 24-345) was used as the search model. PHASER readily found eight Wza monomers in the asymmetric unit which resemble the octameric structure of full-length Wza. Initial attempts to refine the structure using REFMAC^[21] resulted in high R factors (~35%), and led us to analyze the diffraction data with PHENIX.XTRIAGE^[22]. The analysis revealed a possible twinning of the data with twin law k,h,-l and a twin fraction of 0.47. Hence, the twin law along with simulated annealing protocols and TLS groups were included in subsequent refinement rounds with PHENIX.REFINE^[22]. The same refinement protocol was used for sWza and sWza_{Q335C}/MTSSL leading to final R/R_{free} values of 21.5/23.6 % for sWza and 21.5/23.5 % for sWza_{Q335C}/MTSSL. The structure was analyzed and validated using COOT and figures were prepared using PYMOL (<http://pymol.org>).

Crystallographic data

	sWza	sWza _{Q335C} /MTSSL
data collection statistics		
space group	P2 ₁ 2 ₁ 2	P2 ₁ 2 ₁ 2
unit cell (Å)	a=b=140.1, c=165.2	a=b=141.2, c=167.5
wavelength (Å)	1.54	1.54
resolution range (Å)	50.0-3.0	50.0-2.8
mosaicity (°)	0.8	0.6
completeness (%)	99.9(99.7)	99.2(94.5)
redundancy	5.6(4.5)	4.8(2.9)
unique reflections	65664	85823
Wilson B-Factor	65.9	63.8
I/σ(I)	13.8(1.8)	11.8(1.8)
R _{merge}	12.5(89.8)	12.3(63.8)
refinement statistics		
mol./asu	8	8
resolution range (Å)	41.4-3.0	34.5-2.7
R/R _{free} (%)	21.5/23.6	21.5/23.5
rmsd bonds/angles (Å/°)	0.008/1.026	0.007/1.066
Ramachandran (% allowed/disallowed)	99.2/0.8	99.3/0.7
PDB codes	2W8I	2W8H

References